

DISTRIBUTION STATEMENT A
Approved for public release
Distribution Unlimited

19980318 057

DISTRIBUTION STATEMENT A

Approved for public release
Distribution Unlimited

19980318 057

Aspex

Microsystems

REPORT DOCUMENTATION PAGE

Form Approved OMB No. 0704-0188

Public reporting burden for this collection of information is estimated to average 1 hour per response, including the time for reviewing instructions, searching existing data sources, gathering and maintaining the data needed, and completing and reviewing the collection of information. Send comments regarding this burden estimate or any other aspect of this collection of information, including suggestions for reducing this burden to Washington Headquarters Services, Directorate for Information Operations and Reports, 1215 Jefferson Davis Highway, Suite 1204, Arlington, VA 22202-4302, and to the Office of Management and Budget, Paperwork Reduction Project (0704-0188), Washington, DC 20503.

1. AGENCY USE ONLY (Leave blank)		2. REPORT DATE <i>1995</i>	3. REPORT TYPE AND DATES COVERED Final Report	
4. TITLE AND SUBTITLE Near-Earth Object Detection Using the Associative String Processor <i>Requirements Definition</i>			5. FUNDING NUMBERS F6170893W0939	
6. AUTHOR(S) Prof R.M. Lea				
7. PERFORMING ORGANIZATION NAME(S) AND ADDRESS(ES) Aspex Microsystems Ltd Brunel University Uxbridge, Middlesex UB8 3PH, UK			8. PERFORMING ORGANIZATION REPORT NUMBER SPC-93-4059	
9. SPONSORING/MONITORING AGENCY NAME(S) AND ADDRESS(ES) EOARD PSC 802 BOX 14 FPO 09499-0200			10. SPONSORING/MONITORING AGENCY REPORT NUMBER SPC-93-4059	
11. SUPPLEMENTARY NOTES 2 documents: Final report and requirements definition.				
12a. DISTRIBUTION/AVAILABILITY STATEMENT Approved for public release; distribution is unlimited.			12b. DISTRIBUTION CODE A	
13. ABSTRACT (Maximum 200 words) The NEO detection project at Aspex Microsystems Ltd was established to study the feasibility of providing a solution to the NEO problem through a pioneering Modular-MPC (Massively Parallel Computer).				
14. SUBJECT TERMS			15. NUMBER OF PAGES 90	
			16. PRICE CODE	
17. SECURITY CLASSIFICATION OF REPORT UNCLASSIFIED	18. SECURITY CLASSIFICATION OF THIS PAGE UNCLASSIFIED	19. SECURITY CLASSIFICATION OF ABSTRACT UNCLASSIFIED	20. LIMITATION OF ABSTRACT UL	

SPC-93-4059

NEAR-EARTH OBJECT DETECTION
USING THE
ASSOCIATIVE STRING PROCESSOR
REQUIREMENTS DEFINITION

Document Number: 323-001(neo01.wp5/net)

DTIC QUALITY INSPECTED 2

Issue: 1

Date of issue: 6th June 1994

Reproduction in whole or in part is permitted for any purpose of the United States Government

Aspex Microsystems Ltd
University, Uxbridge
United Kingdom, UB8 3PH
Tel : +44 (0)895 274000 ext 2368, Telex 261173G
Facsimile : +44 (0)895 258728

DISTRIBUTION LIST

Lt. Col Marc R. Hallada	(EOARD)
Alain Maury	(O.C.A)
Prof R M Lea	(Aspex)
J Lancaster	(Aspex)
Dr A Krikelis	(Aspex)
Rosh John Joseph	(Aspex)

CONTENTS

1. Introduction	1
1.1 Near-Earth Object Collision	1
1.2 The Impact Hazards	2
1.3 Impact Scenario	4
2. Overview of the NEO Detection Project	6
2.1 Current Search Programs	6
2.2 General Survey Principles	7
2.3 Search Strategy	8
3. Overview of the NEO Detection System	11
3.1 The Detection Hardware	11
3.1.1 The Sensors	11
3.2 The Acquisition Unit	14
3.2.1 The CCD Controller	15
3.2.1.1 CCD Chip Operation	15
3.2.1.2 Imaging Operation of the CCDs	15
3.2.1.3 The Scan Sequence	17
3.2.1.4 The Functional Aspects of a CCD Controller	18
3.2.2 The Preprocessing Unit	19
3.3 The NEO System Controller and Storage	19
3.3.1 The Requirements of the NEO System Controller	20
3.4 The Detection Engine	23
3.5 The Host and User Interface	25
4. Near-Earth Object Detection	26
4.1 Astronomical Image and Model	26
4.2 The NEO Detection Task Sequence	28
4.2.1 Image Acquisition and Image Conditioning	28
4.2.2 Object Restoration and Enhancement	29
4.2.3 Segmentation	31
4.2.4 Analysis	32
4.2.5 Decision	33
5. Conclusion	35
5.1 The NEO Detection System	35
5.2 The NEO Detection Task Sequence	37
5.3 Future Work	38
References	39

1

INTRODUCTION

Asteroids and comets are two distinct classes of bodies that are usually found in the void between the planets. Their small masses and their distinctly contrasting characteristics, suggest that these bodies could have been the "left overs" of the Solar System's evolution and were never incorporated into the planets or their satellites. Thus, remaining in great swarms between the planets and beyond Neptune as asteroid belts and comet clouds. These asteroids are sometimes called minor planets.

Occasionally, some of these bodies escape the confines of these reservoirs of rock, probably through collisions with other asteroids that cause them to be hurtled into the expanse of space. Most of the asteroids or their fragments move into a larger orbit that take them out of the solar system. Erratic orbital change may drive others into an elongated orbit that stretch inwards, across the orbit of Mars and even the terrestrial planets giving them the potential of coming close to the Earth. These potential Earth-approachers or even Earth-threateners are called Near Earth Objects (NEOs). Three classes of such asteroids have been identified namely the Apollo¹, the Aten² and the Amor³ classes.

In March 1989, an asteroid called 1989 FC passed only 1,100,000 kilometres from the Earth. In January 1991, another asteroid, called 1991 BA[2], brushed within only 170,000 kilometres of the Earth (only half the distance of the Earth to the Moon). Such encounters with NEOs have shown that there exists a definite threat of a catastrophic collision. Such an eventuality, real or latent, could alter the course of the planet's very existence.

1.1 Near Earth Object Collision

The occurrence of impacts are very real. As asteroids and other extraterrestrial objects get caught in the gravitational field of a planet, they begin to be pulled towards the planet, passing through its atmosphere before impacting. Such objects that do survive the passage through the atmosphere of a planet to impact are called meteorites.

The Solar System is filled with evidence of impacts. On Mercury and Venus, on the Moon, and on the surfaces of all the moons out by Neptune are pock-marked by impact craters. Geologists, not thirty years ago, did not believe that there were any impact craters on Earth or even on the Moon. However, evidence such as the Barringer meteor crater in Arizona (1.2 kilometres in diameter), the Henbury

¹ Apollo class: asteroids having a semi-major axis greater than or equal to 1.0AU and perihelion distance less than or equal to 1.017AU. Apollo asteroids cross the Earth's orbit at the present time.

² Aten class : asteroids having semi-major axis less than 1.0 AU and aphelion distance greater than 0.983AU

³ Amor class : asteroids having perihelion distance between 1.017 and 1.3 AU. Amor asteroids do not cross the Earth's orbit at the present time

Astronomical Unit (AU) : Average distance between the Earth and the Sun

crater in Australia (0.15 kilometres), the Reis structure in Germany (24 kilometres), or Lake Manicouagan in Quebec (100 kilometres) are all proof of such impacts. Overall, there are some 130 craters or structures around the world that have been convincingly identified as impact craters. In fact, it is now estimated that possibly 26000 meteorites of over 100 grams fall to the Earth each year.

In 1979, physicist Luis Alvarez and his colleagues at the University of California, Berkeley began a debate over impacts when they announced the discovery of a thin layer of Iridium in a geological stratum of the Earth's crust. The layer investigated was significant because it marked the boundary between the Cretaceous and Tertiary epochs, called the K-T boundary, a time related to the mass extinction of the dinosaurs. By the mid-1980s geologists found evidence of Iridium in the same clay layer all over the Earth. Iridium is rarely found on the surface of the earth. These discoveries pointed to the theory that an asteroid of at least 10 kilometres in diameter could have caused such a deposition of the material on impact. Could such an event have triggered the mass extinction at the end of the Cretaceous period?

1.2 The Impact Hazards

The hazards of an impact are very much dependent on the size of the incoming projectile[3] (refer to Table 1) and can be broadly categorised depending on their size or kinetic energy as follows:

Diameter Range (metres)	Period Between 2 Collision in Years	Number of Objects Above Given Diameter	/Area Destroyed In Case Of Collision	Equivalent Number of Hiroshima Bombs
5	10	10 ⁹	None	10 Kilotons
50	200	10 ⁸	Big City	1
200	5000	10 ⁵	State	10000
500	50000	10 ⁴	Country	100000
1000	500000	1600	Continent	10 Million
5000	10-30x10 ⁶	100	Global	?

Table 1 : Scale of Destruction

I. 10 - 100m diameter impactors:

Projectiles in this size range may be crushed or fragmented during atmospheric deceleration, and the resulting fragments are quickly slowed to free-fall velocity, while the kinetic energy is transferred to an atmospheric shock wave released partly as a burst of light and heat. A part is also transported as a mechanical wave. With increasing size, asteroidal projectiles reach progressively lower levels in the atmosphere before disruption and the energy transferred to the shock wave is correspondingly greater. An associated hazard is the possibility that bright fireballs might be misinterpreted as the actual explosion of an actual nuclear weapon.

PROPRIETY INFORMATION

The average interval between impacts of this class may be about 300 years. And 3000 years for such an impact to occur on a populated area of Earth.

II. 100m to 1km diameter impactors:

Incoming asteroids in this class may reach the ground intact and produce a crater. The threshold size is very dependent on the density of the impactor and its speed and angle of entry into the atmosphere. A continuous blanket of material will be ejected from such craters covering tens of kilometres from the points of impact. The zone of destruction extends well beyond this area, where buildings may be damaged or flattened by the atmospheric shock and along particular directions by flying debris. But the total area of destruction could in some instances be less than in the case of atmospheric destruction of somewhat smaller objects because much of the energy that is absorbed by the ground during crater formation.

These objects impact the earth about once per 5000 years and could produce craters of about 2km.

III. 1km- 5km diameter impactors:

Impactors of these size result in catastrophic global consequences. Craters usually 10-15 times the diameter of the impactor are usually formed as a result, is set off. On impact a massive explosion, sufficient to fragment and partially vaporise both projectile and target. Surroundings may be exposed to scorching heat for hours and a continent-wide firestorm might ensue. Dust thrown into the atmosphere would lead to day-time darkness over the whole Earth, persisting for several months dropping global temperatures by about 10 degrees. Months later, the greenhouse effect might follow which would then raise temperatures by 10 degrees. This increase and decrease in global temperatures would severely stress the environment and would lead to a drastic population reduction of both terrestrial and marine life.

The average interval between impacts for this size of impactors is about 500,000 years.

Estimates for the total number of asteroids, based on approximations made from search statistics and lunar cratering record, having diameters larger than values of a particular interest are shown in Fig

1.1.

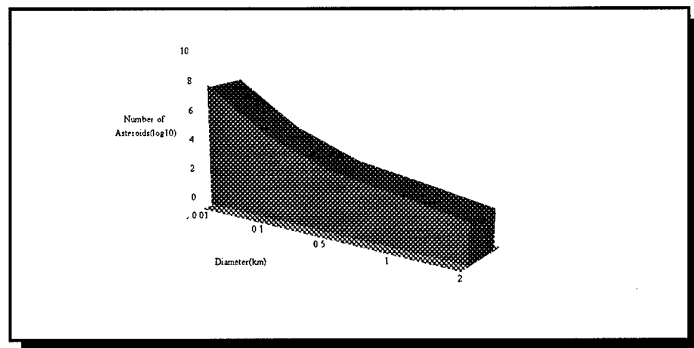


Figure 1.1 Estimated number of Earth-crossing asteroids larger than a given diameter

1.3 The Impact Scenario

John O'Keefe and Thomas Ahrens at Caltech modelled an impact scenario[4]. Using the asteroid 1989 FC , which was about 300 to 400 metres in size and travelling at about 11,000 kilometres per second relative to the Earth (twice as fast of a bullet) in their model, they showed that the asteroid would pass through the lower atmosphere in less than a second; not enough time for anyone in its path to see it coming. A shock wave is then driven into the ground and into the asteroid. The result would be that the asteroid is mostly vaporised changing from solid to liquid to gas in a fraction of a second.

The explosion generated would be equivalent to a 1000 megaton bomb and temperatures would reach about 20,000C. Hot gases from the vaporised objects would shoot into the sky and drag more air with it. A shock wave would then spread away from the impact and everything within a hundred kilometres would be set on fire. About 500 kilometres away the temperature would be a scalding 100C. The blast would travel outwards at 35,000 kilometres per hour, levelling everything for 250 kilometres. Material from the impact would rain down, mostly in the form of molten droplets of rock. A crater about ten times the diameter of the impact would be left behind. Asteroid 1989 FC would have wiped out a city the size of New York in an instant.

If the asteroid were to have struck a 5 kilometre deep ocean, typical of most abyssal plains, a wave up to 5 kilometres high would be driven away from the point of impact. Fifteen hundred kilometres away the tsunami would still be 500 metres high. If such an asteroid were to land in the Gulf of Mexico, the waves would cause flooding in Kansas City.

But whether the asteroid were to hit land or ocean, the dust and soot raised by the impact would cut out the sunlight for months on end, causing an "impact winter" lasting 1000 years. The plume that is sent up into the atmosphere would also carry a wide variety of chemicals that would produce extended periods of acid rain, so much that the acidity of the oceans would destroy almost all marine life.

An impact from even a small asteroid might do little than disrupt the ecosystem for a few years. This could temporarily or permanently effect the agricultural resources that we rely on for food. Calculating the death and devastation from the impact of even an asteroid of barely half a kilometre in diameter, such as 1989 FC, staggers the mind. Such an occurrence would undoubtedly be cataclysmic.

However, near-Earth objects are not the only cause of threat. For the past few decades, man has been sending more and more rockets and satellites into space for the purpose of discovery, for communication and weather forecasting, for military surveillance etc. As times goes by, these

PROPRIETY INFORMATION

equipment would age into functional disuse while continuing to orbit the Earth and in some cases even gradually being pulled back by the Earth's gravitational field. This has resulted in a new threat, that of falling space junk. An NEO detection survey would also help safeguard against such eventualities.

Survey programmes of this type also have other spin-offs of geological and astrophysical significance. The composition of NEOs could give vital clues about the materials from which our Universe was formed. The difference in composition between various types of NEOs would also indicate how material was spread through the Solar System. The orbit of these objects would hint at how the debris escaped from the Solar System. In the future, NEOs could be a potential mining resource. A few near-Earth asteroids are easier to reach (in terms of their differential velocity) than the moon.

OVERVIEW OF THE NEO DETECTION PROJECT

As a first step towards achieving NEO detection and collision prevention goals, a comprehensive inventory of the NEO population should be made. This may be achieved only through a globally co-ordinated long-term search programme with the prime objective of detecting and cataloguing these interplanetary fugitives.

2.1 Current Search Programs

There are currently several independent active search programs undertaken around the world. Systematic search programs like the Planet-Crossing Asteroid Survey (PCAS) and the Palomar Asteroid and Comet Survey (PACS) at the Palomar Observatory, California, USA have been going on for more than a decade. The PCAS program, since its inception in 1973, had the primary purpose of discovering near-Earth asteroids and to determine through a systematic search strategy, the population and the impact rates of planet crossing asteroids. In 1982, PACS was initiated with objectives and techniques similar to PCAS. Both programs use the 0.46m Schmidt⁴ telescope and photographic techniques at Palomar and can independently achieve a combined sky coverage of about 6,000 square degrees monthly. Between the two programs, the average discovery rate has been about 3 per year.

The Anglo-Australian Near-Earth Asteroid Survey (AANEAS) began in 1990 at the Anglo-Australian Observatory, New South Wales, Australia a photography-based 1.2m Schmidt telescope achieving a sky coverage of up to 2,500 square degrees monthly.

An alternative to the photographic search programs was the Spacewatch CCD⁵ Scanning Program, at the Kitt Peak Observatory, Arizona, USA using a Steward 0.9m Newtonian reflector integrated with a CCD detector instead of photographic plates. It differs from the wide-field Schmidt searches in scanning smaller areas of sky but in greater depth. The Spacewatch system presently is discovering approximately as many NEOs as the photographic surveys.

These current programs have achieved a low discovery rate and are proving to be unsuitable in achieving a comprehensive survey of the skies. However, they did contribute to much of the rising interest in this relatively new field of astronomy.

⁴ Schmidt telescope: a type of reflecting telescope (more accurately, a large camera) in which the coma produced by a spherical concave mirror is compensated for by a thin correcting lens placed at the opening of the telescope tube. Providing a wider usable field

⁵ CCD: Charge Coupled Device. A solid state detector used for low-level imaging

In response to the findings of work in the area, NASA was urged to investigate the potential hazards posed by NEOs. Recent NASA international workshops have recommended, through the *Spaceguard Survey* report, on suitable future scientific research and possible strategic defence measures.

These recommendations have been stimulating interest in Europe. Indeed, the EUNEASO (European Near Earth Asteroid Search Observatory) project recently established aims to provide a local network of French, German, Italian and Swedish observatories, as a first step towards the European contribution to a world wide future network, as proposed in the Spaceguard Survey.

2.2 General Survey Principles

A comprehensive survey requires the monitoring of a large volume of space to discover asteroids and comets whose orbits could bring them close to or even pass the Earth's orbit. Such bodies can be distinguished from main-belt asteroids by their differing motion in the sky and, in the case of comets, by visible traces of activity. The basic objectives of such an NEO survey can be summarised as follows:

- A. to find most of the larger and potentially dangerous NEOs
- B. to calculate their long term orbital trajectories
- C. to identify any NEOs that may impact the Earth over the next several centuries.

These fundamental objectives in turn relate to secondary objectives more aligned towards the detection system. A detection system should have as its main aim the maximisation of the discovery rate. Hence

- I. sufficient primary, independent sky coverage is required to increase the likelihood of detection.
- II. have a quick look strategy to inspect data in real-time, so that discoveries may be quickly and reliably confirmed.
- III. intensive, collaborative astrometric follow-up of the new discoveries to obtain sufficient orbit accuracy to facilitate recovery at subsequent apparitions.

The discovery rate is dependent on the number of available asteroids at a given limiting magnitude⁶ and is proportional to the primary sky coverage obtained. Primary sky coverage is governed by the telescope's field of view and the efficiency of the detector. The latter is determined by the "speed" of the optics and the intrinsic properties of the recording medium. This is expressed in practical terms as the exposure time or minimum frame rate.

⁶ magnitude(astronomical): a number, measured on a logarithmic scale, used to indicate the brightness of an object

Another consideration is the limiting magnitude of the telescope/detector combination. A fainter threshold for detection seems desirable in that the search volume is increased and fainter objects are sampled. To achieve a fainter threshold, larger aperture telescopes and/or more sensitive detectors are required. However, both of these requirements are usually associated with a smaller field of view which could nullify the advantage of greater search sensitivity by drastically reducing sky coverage.

To achieve search objectives, it is necessary to have a means of quickly discriminating the potential "target" images from the "noise" represented by the vast number of main-belt asteroid images detected. To ferret out these objects would require a comprehensive program of astrometry. Given a required minimum sky coverage and the rapid follow-up program requirement of the directed search, such a program becomes prohibitively difficult. The degree of completeness must hence be compromised in order to satisfy the objectives.

2.3. Search Strategy

A model of a whole-sky survey[3] with 2,100 ECAs⁷ larger than 1km, 9200 larger than 0.5km and 320,000 larger than 0.1km and also a sample of 158 ECCs⁸, observed during the last 100 years, was simulated to understand how a survey could be optimised. The model also incorporated corrections in detection, biased due to observational selection (which favours objects that bring them often into near-Earth orbits) and reflectivities of the bodies' surfaces (which favours bright objects over dark ones). Also losses due to trailing, confusion with main-belt asteroids and confusion with stars and galaxies were also taken into account.

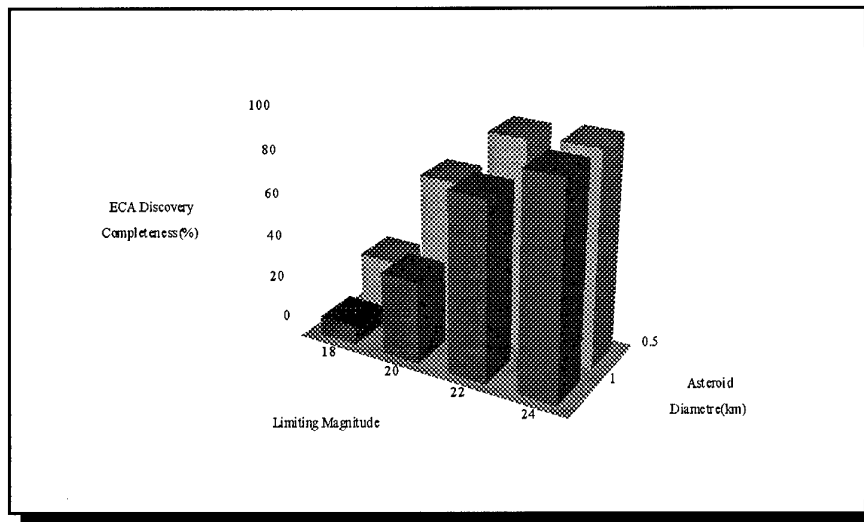


Figure 2.1 ECA discovery completeness for sky surveys lasting 25 years

⁷ Earth-crossing Asteroids: An asteroid whose orbit crosses the Earth's orbit or will at some time cross the Earth's orbit as it evolves under the influence of perturbations from Jupiter or other planets

⁸ Earth-crossing comet: A comet whose period is greater than 20 years and perihelion distance is less than 1.017AU

To achieve greater completeness and therefore greater levels of risk reduction, it was found that larger telescopes with fainter limiting magnitudes were necessary. This can be seen in the graph in Fig. 2.1 which demonstrates the discovery completeness of whole-sky surveys over a period of 25 years against the limiting magnitudes of objects searched for. With limiting magnitudes less than 24, 100 % discovery completeness may only be achievable for sky surveys lasting much longer than 25 years.

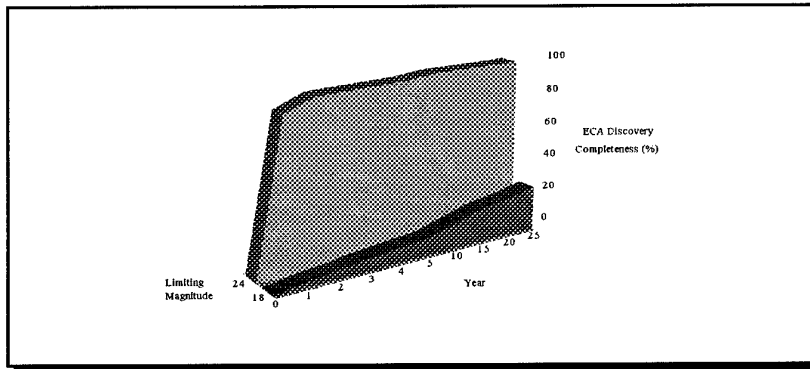


Figure 2.2 Rate of ECA discovery for limiting magnitudes of 24 and 18

It was also seen, that at faint limiting magnitudes, there is a rapid decline in the discovery rate of ECA's which makes increasing the duration of the survey inefficient. This can be seen in Fig. 2.2 showing detection rate between surveys with limited magnitudes of 24 and 18 for objects with diameter of 1km. After a rapid initial detection rate for a survey with limiting magnitude of 24, it is followed by a much slower approach towards completeness. From the survey model, 90% of objects would be detected by the first year of the survey for a limiting magnitude of 24 while for a limiting magnitude of 18 only about 3% of objects were found.

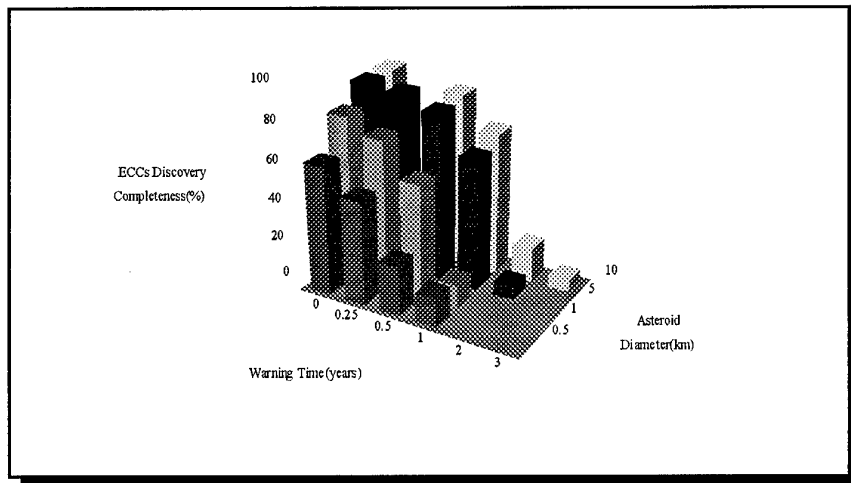


Figure 2.3 ECC discovery completeness with respect to the required warning times

PROPRIETY INFORMATION

The sky survey models for EECs also revealed that for adequate warning times a compromise of discovery completeness would also have to be made as shown in Fig. 2.3. Search areas in the range of 5,000 to 10,000 square degrees per month were found to provide only two-thirds discovery completeness with 500 ECA discoveries during the first month. This high initial discovery rate would then gradually tail off by a factor of two over the course of 25 years.

Not only did the simulations of a survey model show the need for increased sky coverage for fainter limiting magnitudes and hence suggest the requirements for the primary detection systems (i.e. the optical aspect of the system) but it also revealed the requirements for the secondary detection system (i.e. the system responsible for the processing of the images obtained). With photography-based surveys, the digitisation of photographic plates was necessary before computers could be used for the processing. Thus, introducing delays in acquiring results. However, even with a fully digitised system, as in the Spacewatch program[5], where CCD chips captured the image in a digitised format before being read out to be processed on a Solbourne 5/600 workstation, with three 62-bit processors, (scaleable architecture SPARC chips) only near real-time performances could be achieved. The Spacewatch survey could only estimated a 2.2 times increase in discovery rates over its photography-based counterparts such as PACS (with a discovery rate of ~6 objects/year).

These figures show the inept performances of the current survey programs, as compared to the requirements introduced by the simulations. Increased sky coverage may be achieved by the use of an integrated network of telescopes all over the world. Thus, providing a cost-effective solution by utilising already available optical hardware. However, the secondary detection system would have to be much more powerful than the Spacewatch workstation to be able to provide the processing muscle that could handle the computation-intensive and data-intensive requirements for the detection of near Earth objects. It is apparent that to meet such objectives a system that has as its detection engine a parallel computer would be ideal in fulfilling the needs of a survey program.

3

OVERVIEW OF THE NEO DETECTION SYSTEM

This chapter discusses the functional requirements for an NEO detection system. Examples of such systems and designs are already in evidence in the Spacewatch program at Kitt Peak, Arizona, USA and the NEO detection project at the Observatoire de la Cote d'Azur (O.C.A), France. Though the specifics of the such systems differ their functionality and principle are similar.

3.1 The Detection Hardware

An overall synopsis of the functional aspects of an NEO detection system, as pixel data is transformed into image data and then to the output of detected objects, is illustrated in Figure 3.1. It basically comprises of 7 basic blocks: the sensors, the acquisition unit, the NEO system controller, the image storage, the NEO detection engine and the host and user-interface.

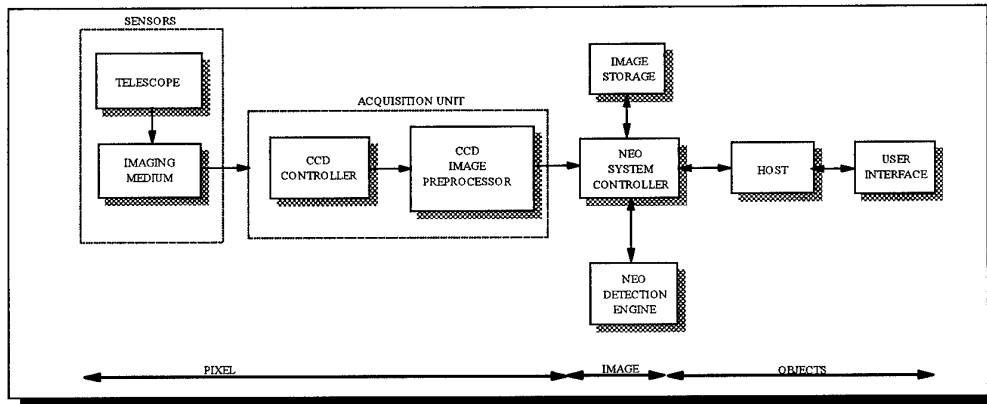


Figure 3.1 Block diagram of an NEO detection system

3.1.1 The Sensors

Sensors actuate the transfer of real world information into forms that can be used digitally for required processing. For the application of NEO detection, the sensors generally consist of a telescope and an imaging medium, e.g. photographic plates and CCD chips.

For the purpose of an astronomical survey, wide aperture telescopes provide a large field of view necessary to accomplish survey objectives. Such telescopes would also improve the efficiency with which areas of the sky are searched. For example, a typical Schmidt telescope has a field of view of

6.5 to 10 degrees compared to the 40 arc seconds of the 0.9m Newtonian Spacewatch Telescope at Kitt Peak, Arizona. Indeed, Schmidt telescopes are ideal for conducting a sky survey.

Most telescopes use photography as an imaging medium. However, in the past few years the use of photography has faced a descendency to charge coupled devices. This is because photography has proved to be inefficient and unsuitable for capturing astronomical images.

The comparison of photography and charge-coupled devices for the characteristics given above is shown in Table I. It shows that in all cases but one CCD sensors perform better than photography. A good imaging medium should have the following characteristics[6]:

1. *Resolution*: It reflects on its ability to see fine detail. Hence, the resolution should be as high as possible.
2. *Detective Quantum Efficiency (DQE)*: It provides a measurement of the amount of radiation actually detected by a sensor, given the total amount of radiation falling on it. The DQE should be high.
3. *Operational Detective Quantum Efficiency (ODQE)*: The ODQE gives a measurement of the efficiency with respect to the acquisition time and the time before sensor information can be interpreted. The ODQE should be high.
4. *Spectral range*: The sensitivity of the sensor to different wavelengths is an important property for a sensor. A broader range would allow the same sensor to reveal characteristics of an object in different wavelengths.
5. *Dynamic range*: This gives the difference between the brightest and faintest objects that can be detected simultaneously and should be as great as possible
6. *Detector stability* :The sensor should be stable over long periods of time such that it produces the same output signal for the same input signal over the same given time.
7. *Linearity* : The output should be linear, i.e. if one object is twice as bright as another, then the output should be twice as bright.

Properties	Photography	Charged-coupled Devices
Resolution	High	Moderate
DQE	~10%	~80%
ODQE	Low	High
Spectral Range	Visual spectrum	X-ray to Near Infrared
Dynamic Range	~100	~100000
Stability	Poor	Good
Linearity	Poor	~0.1%
Photometric Accuracy	5%	0.5%
Surveying Efficiency	Moderate	Moderate

Table I Comparison of photography and charged-coupled devices

8. *Photometric Accuracy* : The sensor output should be in such a form that the brightness of an object sensed can be easily measured with high precision in absolute units, such as magnitudes.

9. *Surveying Efficiency* : This is characteristic that is specific to an application of surveying. It gives a measure of efficiency of detection given sensor size and is calculated as shown below.

$$\text{Surveying Efficiency} = \text{DQE} \times \text{sensor detection area}$$

Photographic emulsions are only suitable in detecting very bright, near or slow moving objects due to its low DQE. As photographic plates have to be removed from their slots in the telescopes to be developed before any analysis of the images can be done, the time between acquisition and interpretation can extend from a few hours to a few days. This results in its low Operational Detective Quantum Efficiency(ODQE). In CCDs, however, interpretation can begin almost immediately after the image is captured by the sensor. Also the ease with which the captured images can be digitised provide the potentiality of using powerful computers in operations related to acquisition and analysis. Thus, real time can also be achieved with the use of such computers. Thus , improving its ODQE.

The large spectral capabilities of the CCD sensor allow it to be used in interesting applications. For example, since the energy (or wavelength) of impeding radiation can be directly measured by the amount of charge, an X-ray astronomer could obtain simultaneous high resolution spatial and spectroscopic data by subjecting the CCD to superimposed short exposures .

The large dynamic range that CCD sensors are capable of allow contrasting objects to be imaged on the same field. This is particularly important in an astronomical detector because of the large brightness differences found within an object (e.g. a galaxy nuclei and its outer parts) and between objects.

The remarkable linearity and stability of CCD chips offer a more homogenous background, a more regular point-spread function and allow for the compensation of pixel-to-pixel variation. Though the physical sizes of CCD chips are small, their surveying efficiency per chip would be comparably lower than photographic plates. This can, however, be increased by only using a mosaic of CCD chips to increase the survey area, as the possibility of increasing detecting areas of single CCD chips are constrained by size, yield limits of crystal growing and semi-conductor processing.

Multi CCD array sensors are usually arranged as a staggered array as shown in Fig 3.2. The staggering of CCDs is done primarily because CCD packaging extends from the main pixel area making it physically impossible to allow a continuous coverage when CCDs are placed side by side.

Also, on observing an area of the sky, the full image as seen by the CCD mosaic should be such that information is not lost at the boundaries between separate CCDs. The result of this is a requirement for the overlapping of the individual CCD fields such that even the largest object will not be lost. The amount by which the CCD chips are overlapped would be dependent on the expected maximum object size to be detected. For the NEO detection project[7] such an object is assumed to be 15 pixels in width. A staggered arrangement of the CCDs with an overlap of 15 pixels along the y-axis and a distance of $(2048 - 2 \times 15)$ pixels along the x-axis is required as shown in Fig 3.2.

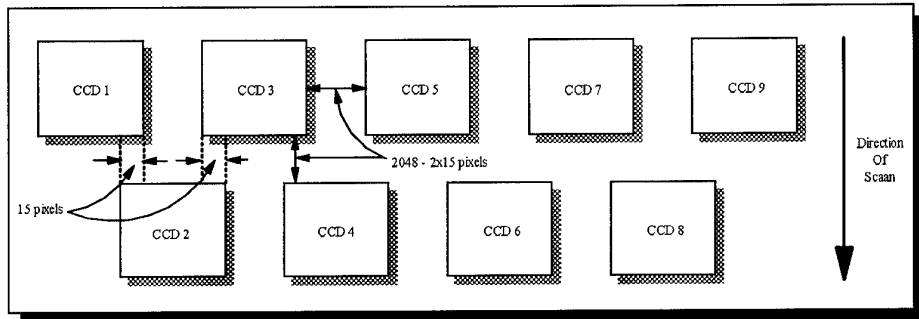


Figure 3.2 The staggered layout of a CCD mosaic

An example of CCDs that have been considered for the purpose of detection in the NEO project are the Loral and Kodak CCD chips. A comparison of the characteristics that are usually taken into consideration when making a choice between different CCDs are given in Table II. From the table, the Kodak CCDs appear to be better suited to the task due to its smaller size, angular resolution, the number of read-out registers and full well potential as compared to the Loral.

Brand Name	Loral	Kodak
Size	2048x2048	2048x2048
Pixel Size(microMeter)	15	9
Physical Size(mm)	30.72	18.43
Angular Field of View	33.42'	20'
Number of CCD Chips/ 30cm	9	16
Pixel Scale	0.979"	0.587"
ReadOut Register	1	2
Full Well Potential	150,000 e-	85,000 e-

Table II Comparison of the Loral and Kodak CCD chips

3.2 The Acquisition Unit

The main functionality of the acquisition unit is fundamentally to control the read-out of sensed data from the CCD and to transform it into a form that is compatible for processing in later stages. This acquisition and transformation of data is dependent on the operational aspects of the CCD, the

method by which the CCD will be used and the amount of data that has to be handled by the system. As seen in Fig. 3.1 the acquisition unit has two main functional blocks : the CCD controller and the pre-processing unit.

3.2.1 The CCD Controller

The design of the CCD controller is dependent on the CCD's operating characteristics and the way in which it is used.

3.2.1.1 CCD Chip Operation

CCD imagers operate on four sequence of steps:

1. Photoelectron Generation : This is the conversion of incident light into a proportional quantity of electrical charges (electron-hole pairs).
2. Electron Collection : These charges are then collected at gates that are fundamentally capacitors.
3. Charge transfer : These charges have then to be read-out sequentially along these gates in a row.
4. Read-out : At the end of each row is an output register that then transfers these collected charge packets to an output amplifier to be converted into an electrical voltage.

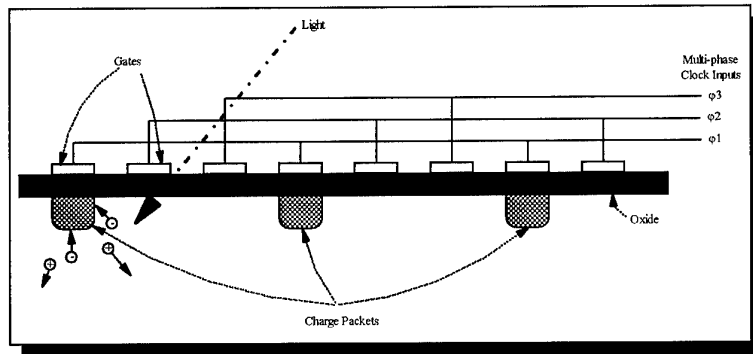


Figure 3.3 CCD chip operation

3.2.1.2 Imaging Operation of the CCDs

A CCD array would be housed in the focal plane of the telescope and can be used in three basic modes: the sidereal scan mode, its variant the fast scan mode and the stare mode. The two main modes are illustrated in Fig. 3.3. The timing constraints of the system is very much dependent on the mode in which the CCDs are used for observations and the objects that are to be detected.

Sidereal Scan Mode

The sidereal scan mode is implemented by utilising the rotation of the Earth while keeping the telescope at rest. The rotation of the Earth causes the image of the star to drift across the detector. However, if the CCD is clocked synchronously with this rotation such that accumulated packets of charge remain below the star during its transit, then the integrity of the image can be maintained. The image can then be read-out from the amplifier at the tail of the scan motion. Only one amplifier can be used in this mode. Such a scan mode also produces images that are independent of the effects due to sensitivity differences between pixels and thus flat fielding calibrations are not needed.

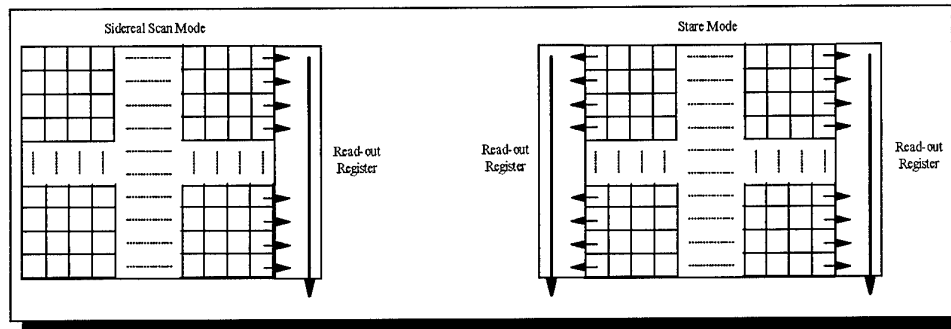


Fig. 3.4 The different scan modes : Sidereal scan and Stare mode

Though this scan might provide limited control requirements for the telescope motion, the sidereal scan requires different clocking rates between the bottom and top pixels. This difference increases when the area of scan is lower down in the sky.

The limiting factor in this mode is thus the sidereal speed (i.e. the rotation of the Earth). For an object that begins at the starting edge (i.e. at the head of the sidereal motion), it would take 133 seconds for it to reach the edge at which it could be read-out for a Loral CCD. Thus, the read-out time per CCD would be about 15 lines/sec. This speed is easily achievable by the electronics of the acquisition unit. In fact, the acquisition unit enters a wait state before the next line is available for read-out. To improve the efficiency of the system as a whole, these wait states can be reduced by moving the telescope in the direction of the sidereal motion thus requiring a faster read-out and hence result in a reduction of wait states. The limiting factor in this case is the speed at which the electronics can work. This is the *fast scan* mode. The advantage of this mode is that a larger area of the sky is surveyed. The disadvantage, however, is that the detection is not very deep and is not suitable for fast moving objects.

The Stare Mode

This mode represents the easiest solution to a scan mode. Here the CCD is exposed to an area of the sky for a period of time dependent on the type of object to be detected. The CCD is then read out and the telescope is repositioned for the next exposure.

The exposure period is proportional to the distance of the objects from the Earth. Main belt asteroids require an exposure time of 2-3 min while far asteroids require 10 min. The time to reposition the telescope is approximately 10 sec. Existing read-out times from the Loral CCD (as implemented at O.C.A, France) is about 55-110 sec. Thus the minimum time⁹ per CCD is less than 185 sec.

3.2.1.3 The Scan Sequence

Each CCD field of view has to be taken at least 3 times for any effective detection to be carried out. A scan sequence along one direction is done to give approximately 20 exposures as seen in Fig. 3.5 before returning to the field for the first scan and is repeated three times to give three views of the same area. By accurate astronomical co-ordinate reduction and registration, for each of the frames in the three scans, the astronomer obtains three different position of the detected objects can be classified and from which the trajectories and the characteristics of the asteroid can be calculated.

Such a scheme, of requiring three separate passes, could be avoided if two or three staggered rows of CCD chips are used. Since the same field will be covered by the staggered rows one after the other as it moves along the direction of scan, three views of the same field are automatically made.

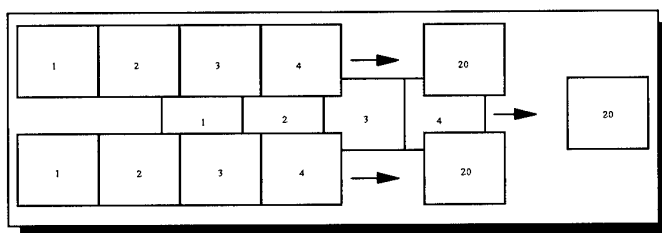


Fig 3.5 The coverage of a scan sequence for a 3 CCD chip mosaic with 20 exposures.

In these modes the performance expected from the mentioned CCDs and their related circuitry are shown in Table III.

⁹ Minimum Acquisition Time = Exposure Time + Repositioning Time + Read-out Time = 2 min + 10sec + 55 sec. Since read-out can begin immediately after exposure and during repositioning of the telescope

PROPRIETY INFORMATION

Brand Name	Loral		Kodak	
Scan Mode	Sidereal	Fast	Sidereal	Fast
Estimated Limiting Magnitude	21.7	19.7	21.2	18.7
Square Degrees Per Hour	75.6	398.9	80.2	508.8
Kilobytes Per Second	62.8	333.3	105	666.6

Table III CCD scan characteristics

3.2.1.4 The Functional Aspects of a CCD Controller

A typical functional block diagram of a CCD controller[10] is shown in Fig. 3.6. The transfer is achieved by multi-phase clocking inputs applied to the gates in such a way to transfers the data along the row as packets as in Fig 3.3. A two phase clock effectuates a transfer in only one direction. Bi-directional transfers may be achieved by three phase structures. Such bi-directional capabilities are desirable for large area segments, as this would effectively partition the CCD into two segments to achieve faster read-out capabilities. For proper operation, these charge transfer operation is to be carried out in the dark. Hence, the sensor would have to be strobed .

Timing(logic) circuit and wave shaping(driver) circuits are required to handle these operations. Low timing jitter is essential in CCD operation which is best provided by a periodic digital pulse generator derived from a stable source e.g. a crystal controlled master clock. A high speed dedicated processor may be used to control a programmable, stable timing chain. Thus, retaining the flexibility of software timing while providing the stability needed for low noise CCD operation. Also the need for differential clocking rates between lines at the top and bottom of the CCD can be more easily realisable.

In a few of the CCD controllers that have been designed, as in the Steward Observatory, Arizona and at O.C.A, France, DSP chips have been used for this purpose. The DSP, found to be quite a cost-effective solution, is used to generate the required waveforms via an appropriate micro-store and D/A converters. Before these logic signals may be applied to the CCD they have to be conditioned, by the driver circuits, to well-defined upper and lower pulses with low noise and minimal overshoots during a transition.

The read-out signal extracted from the CCD are analogue outputs. Pre-amplification of these CCD signals are necessary. Due to the effects of noise, capacitances within the CCD chip and feedthrough components of pulses from other parts of the chip the signals have to be conditioned before being passed into the ADC.

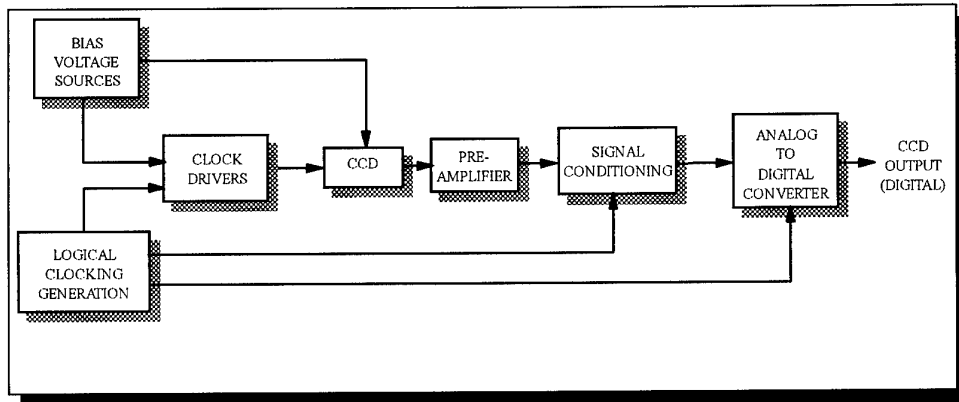


Fig. 3.6 Functional block diagram of a CCD controller

3.2.2 The Preprocessing Unit

This unit provides the interface to the rest of the detection hardware. Such a unit would comprise of an amplifier stage, a data truncater (depending on the resolution provided by the A/D) to obtain byte-multiple pixel sizes e.g. 18 to 16 bit truncation, and serial-to-parallel conversion circuitry. If the preprocessing unit is based on a powerful processor, then, the necessary pixel conditioning to remove CCD- pixel defects and anomalies can be undertaken at this stage. Operations like the dark and flat fielding calibration can be done on-the-fly to normalise individual pixel sensitivity.

3.3 The NEO System Controller And Storage

The NEO detection system controller is functionally central to the overall system and has thus, several tasks. It provides the global control and synchronisation to the acquisition unit. Also, it is at this point that the integration of acquired pixel data, from respective CCD frames, into an image takes place. The controller handles the back-up storage of images, whether in buffers, before being processed, or in secondary storage devices. It is responsible for data transfers to the detection system and also the output of results to the host and hence, to the outside world.

The requirements of this aspect of the detection hardware can be better understood by looking at the problem of an astronomical survey, and hence the amount of data that would have to pass through the NEO system controller

3.3.1 The requirements of the NEO system controller

For a comprehensive asteroid survey, search areas in the range of 5000 to 10,000 square degrees[3] would be necessary to make it plausible. It is practicable to observe a region extending as much as +/-120 deg celestial longitude from opposition and +/-90 deg celestial latitude. Thus, giving a search coverage of about 43200 square degrees. The complete sky is not surveyable throughout the year due to the presence of bright astronomical bodies that would make observing a particular region of the sky impossible during certain periods of the year.

Consider a CCD mosaic that would survey 6000 square degrees per month. In a month only a maximum of 20 days of 8 hours each are suited to observation[13]. Given the details of the two CCDs considered in Table II and Table III, an idea of the volume of data to be acquired, processed and catalogued is presented in Table IV.

Brand Name	Loral			Kodak		
Number of Bytes/Exposure	8.4 MBytes			8.4 MBytes		
- For 1 CCD	8.4 MBytes			8.4 MBytes		
- For a mosaic in a 30cm focal plain	75.5 MBytes (9 CCDs)			134.2 MBytes (16 CCDs)		
	Sidereal	Fast	Stare	Sidereal	Fast	Stare
Observed Sq. Deg./Hour	75.6	398.9	41.9	80.2	508.8	34.6
Acquisition Time(sec)	133	25.2	240	79.8	12.58	185
CASE I						
Observed Hours/Month (for 6000 sq. deg. of coverage/month)	79.4	15	143.2	74.8	11.8	173.4
No. of Exposures	2,149.2	2,142.9	2,148	3,374.4	3,376.8	3,374.3
Volume of Data (Gigabytes/Month)	162.2	161.8	162.2	452.8	453.2	454.8
CASE II						
Observed Hours/Month (for all 20 days in a month)	160	160	160	160	160	160
No. of Exposures	4,330.8	22,857.1	2,400	7,218	45,787	3,113.5
Volume of Data (Gigabytes/Month)	327	1,725.7	181.2	968.7	6,144.6	417.8

Table IV Volume of data to be processed for a survey with a CCD mosaic in a 30 cm focal plane, as found in the Schmidt telescope at O.C.A, France

Although in Table IV, the fast scan mode in both the Loral and the Kodak CCDs show a reduction in data volume in case I, this is only because an upper limit of 6000 square degrees was taken in the calculations. However, in reality as shown in case II, fast scan modes are used to increase the coverage of the survey, hence much larger data volumes can be expected.

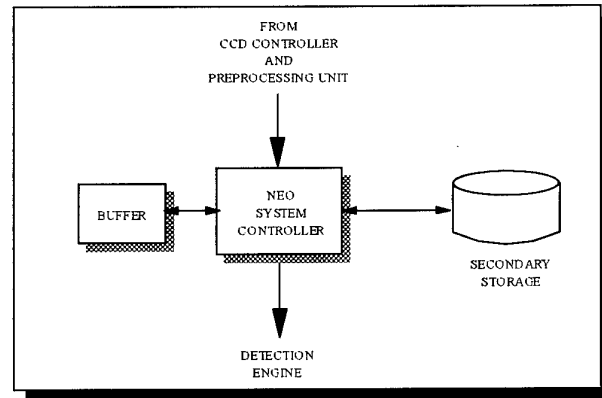


Fig 3.7 The NEO system controller and storage

These massive volumes of data, in whichever mode, would have to be stored appropriately while maintaining the integrity of individual CCD frames. Storage would have to be achieved at two levels : a temporary buffer to be used as a transit point towards the detection engine and a secondary storage facility for archiving as illustrated in Fig. 3.7.

The temporary storage facility may be implemented as either a single or a dual buffer. The method of implementation is dependent on several factors, namely, the method of scan , the I/O bandwidth of the detection system, the computational power of the detection engine and the way in which the acquired data is to be processed.

In the stare mode the full image is available before the CCD chips can be read-out. If a single buffer is to be used then processing on these frames would have to be achieved within the exposure time (79.8 sec for a Kodak CCD). While with a dual buffer, processing time would be equivalent to the total acquisition time as calculated in section 3.2.1.2. Hence, reflecting on the detection system performance requirements.

In the sidereal and fast scan modes, images can be handled as either a whole or as a collection of lines. Whether the processed data is a whole image or a collection of lines, the continuous scanning would require that a second buffer be available to store incoming data while data stored in the other is processed. The processing of a collection of lines introduces a requirement for a complex control, to allow for the overlapping of lines between different collections necessary for faithful image processing.

With a large mosaic CCD imaging system, necessary for NEO detection, the acquisition synchronisation and the expected transfer rates (between 0.5-10 Mbytes/sec are shown in Table V), suggest a need for a hierarchical multi-controller schematic as the most cost-effective solution. Such a schematic would comprise of an individual CCD chip or a sub-array of CCD chips serviced by a

local acquisition unit and controller, and a master controller then servicing a group of these units. This arrangement would imply the need for multi-channel controllers as seen in Fig. 3.8.

Brand Name	Loral			Kodak		
No. Of CCDs in a 30 cm focal plane	9			16		
Number of Bytes/Exposure	75.5 MBytes			134.2 MBytes		
	Sidereal	Fast	Stare	Sidereal	Fast	Stare
Acquisition Time (sec)	133	25.2	240	79.8	12.58	185
Transfer Rates (Kbytes/sec)	567.7	2,996	314.6	1,681.7	10,650.8	725.4

Table V Transfer rates for a mosaic CCD in a 30 cm focal plane

With this scheme, the local controllers would be primarily responsible for controlling the acquisition of CCD data from the sub-array and also handle the temporary storage of individual frames in their individual local buffers. It would also handle the archiving of these images on secondary storage systems. The synchronisation of these local sub-array controllers and hence the acquisition of the entire array of the sensor would be managed by the array controller. The array controller would have to maintain the integrity of the overall composite image and allow access to the data by the detection engine.

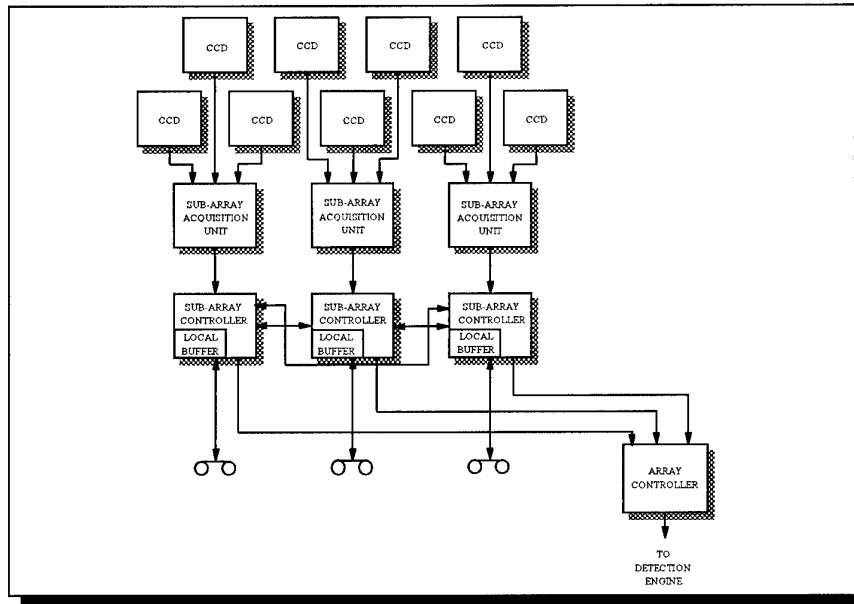


Fig. 3.8 Hierarchical multi-controller schematic for a large array CCD imaging system

Multi-controller systems of this sort provide the possibility of increasing the number of CCD chip that may be used by the imaging system and hence improve the detection rate by increasing search area. Also, independent controllers allow real time detection to be implemented.

3.5 The Detection Engine

The detection engine, as seen in fig 3.1 has as its functionality the detection and recognition of objects in the image. The detection engine processes the calibrated data, available in the buffers of the acquisition controller (sub-array controller) to give a list of detected near-Earth objects. These operations have to be carried out on the massive data volume that is generated by the CCDs. The figures in Table IV, give an idea of the amount of data that would have to be worked on. The larger the survey area, the more efficient the survey becomes as seen in section 3.1.1. More objects would hence be detected and recognised.

The task of image processing is a computation-intensive and data-intensive problem. Also, for the purpose of NEO detection the image processing rate scales linearly with the number of objects detected per second. Sequential processing on a digital computer provides the cheapest solution to any image processing requirement. However, such an approach is not optimal, due to inherent limitation in the underlying architecture of a sequential computer, resulting in a very large number of operations because of subsequent pixel-by-pixel processing involved.

To put this requirement into perspective, consider the Solbourne workstation integrated with Spacewatch Telescope with a single 2Kx2K CCD chip at the Steward Observatory, Kitt Peak, USA, that is used as the detection engine, with 3 64-bit scalable-architecture Sparc processors. It has been estimated that it can detect up to 10,000 objects in a 165 sec exposure giving an object rate of 60 objects/sec. At a limiting magnitude of 22, detection of about 30,000 objects/square degree is estimated by the Spacewatch Telescope.

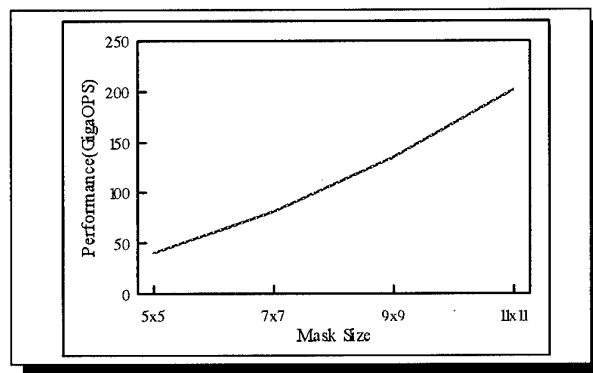


Fig. 3.9 Computation requirements for a simple detection algorithm involving a spatial filter(noise removal) and a maxima detection operation(object location) using different mask sizes on images from a mosaic of 16 Kodak CCD chips used in the sidereal mode.

If a detection system with 16 Kodak CCD chips were used in a sidereal scan mode and, for simplicity, a detection algorithm consisting of an $n \times n$ spatial filter ($[n \times n]-1$ addition operations) and a maxima detection operation in an $n \times n$ window ($[n \times n]-1$ comparison or subtraction operations) were to be used as an initial stage for NEO detection, an idea of the number of operations involved can be obtained. These operations would have to be achieved in 79.8 sec as seen in Table IV. Then, Fig. 3.9 demonstrates the performance requirements for the NEO system which could easily exceed 0.5 TeraOPS.

Assuming a similar detection rate of 30,000 objects/ square degree, then, given a pixel scale of 0.578" for the Kodak CCD, the total survey area,

$$\left(\frac{0.587}{60 \times 60}\right)^2 \times 2048^2 \times 16 = 1.78 \text{ square degrees}$$

Hence, the number of objects that will be detected,

$$30000 \times 1.78 \approx 53527 \text{ objects}$$

Each object would then have to be manipulated after the initial detection stage, requiring more computation. Given the detection rate for the Solbourne workstation, the time to detect 53527 objects would be

$$53527 \div 60 = 892.1 \text{ sec} \approx 15 \text{ min}$$

Such performances would be unacceptable and real time detection would be impossible. These requirements would definitely demand a high performance engine. This can only be fulfilled by a massively parallel processor.

Besides the requirements on processing performance, other important constraints also exist. As telescopes get bigger, more and more CCDs will be fitted into the focal plane to increase the coverage of the survey. Hence, the massively parallel processor should be scaleable to accommodate possible expansions of survey coverage to meet the increase in processing performance requirements.

Also, the mechanical and physical requirements of the astronomical environment (i.e. telescope and the remote observatory locality), the engine should be suitably small, reliable and cost-effective. Also the programmability of such a machine would be an advantage, providing an acceptable gradient in the learning curve. The cost of replicability is also a factor that would effect the possibility of similar machines being set up in observatories around the world.

These requirements; namely size, weight, power, cost-effectiveness, scalability, reliability, programmability and replicability, seem to suggest the Associative String Processor(ASP) as a suitable choice.

The ASP is a second-generation, scalable, fine-grain Single Instruction Multiple Data (SIMD), massively parallel processor[15], allowing exploitation of both control and data level parallelism, content matching and dynamically reconfigurable inter-processor communication. Advances in microelectronics has also allowed highly compact, fault-tolerant and cost-effective modules to be produced.

The flexibility and adaptability of the ASP to differing problem domains have been demonstrated, through research emerging at Brunel University and Aspex Microsystems Ltd, by its performance in two DARPA-sponsored Image Understanding benchmarks in comparison with other contemporary parallel architectures were extremely encouraging and also, its evaluation for the On-board Signal and Data Processing scenario of Time Dependent Processing and Object Dependent Processing sponsored by the Rome Laboratory. The ASP has also been proven to be cost effective in space-based application in a number of projects funded by BMDO (formerly SDIO). A number of ASP prototypes have been built and four are currently being used based-on CERN (European Centre for Nuclear Research) collaborations. The target cost-effectiveness being approached by the ASP, over a number of technology research and development, may be summarised[16] as

performance/size ratio	:	1 Tera-OPS/ft ³
performance/weight ratio	:	0.1 Tera-OPS/lb
performance/power ratio	:	1 Giga-OPS/W
performance/cost ratio	:	10 Mega-OPS/\$

where an OPS is the time for a 12-16 bit addition

3.5 The Host and User Interface

A host facility in fig 3.1, gives the necessary interface to astronomers in the control of the entire NEO detection operation and hence, should be at the top end of such a system. Also through such a host, information regarding detected NEOs can be communicated to the astronomical community via existing global networks like the Internet. Such a facility would be essential when follow-up tasks are essential in confirming dubious objects by other observatories around the world.

A graphics display routine could be considered for the CCD images within the integrated real-time detection system but this is only a secondary or cosmetic requirement. This is because at the moment a list of possible NEO objects with appropriate co-ordinate location and trajectory information would suffice as a survey objective.

4 NEAR-EARTH OBJECT DETECTION

The detection of near-Earth objects involves the extraction of astronomical objects from images obtained from the CCD camera mounted on a telescope and the recognition of these objects to give a possible list of asteroids that could then be classified as Earth-approachers or Earth-crossers. The recognition and classification of astronomical objects as NEOs are based on the motion of these objects through space. Non-stationary objects may be established either by streaks found in the images or by the comparison of frames of the same field to observe objects that steadily drift from frame to frame. The latter form of detection is the most likely criterion that would be establish the presence of NEOs.

Several techniques for astronomical object detection are already available in programs like the Spacewatch program, DAOPHOT¹⁰, FOCAS¹¹ etc. In the Spacewatch program, NEO classification is achieved by a two stage task sequence of streak detection and motion detection. Complex and precise such as in the DAOPHOT program[17] are available for utilisation for the detection of astronomical objects. However, though fundamental principles are similar, such precise reduction of images are over-justifiable in satisfying the objectives of detection. As the confirmation of the presence or absence of NEOs are made by frame comparison, errors in the accuracy of photometric reductions due to the point-spread function of the optical system or cosmic rays are made negligible, since these parameters are more or less constant between frames, all taken in a short period of time. This is achieved by ensuring that the object of concern is the same, in characteristics, between frames.

4.1 Astronomical Image and Model

Most image processing solutions are based on an approach that is based by an image model that would best represent the characteristics of the object of interest to aid in its detection or recognition. At this point, the inventory of an astronomical image should be mentioned so as to provide a better understanding of previous and present image models in astronomy.

An astronomical image generally includes the following objects

1. **stars** : differing in brightness having a gaussian intensity profile. Their sizes range from 2 to 4 pixels wide
2. **galaxies** : appear as "blurred" stars, with sizes much larger than stars and are usually elliptical in shape
3. **diffuse nebulae** : having any shape but generally with sizes above 5 pixels.

¹⁰DOAPHOT : Dominion Astrophysical Observatory program for crowded field stellar PHOTometry

¹¹FOCAS : Faint Object Classification and Analysis System

- 4. **asteroids** : appear star-like or as trailed images(streaks) of similar size to stars
- 5. **comets** : appear as fuzzy bright objects with or without a tail
- 6. **cosmic rays** : appear as sharp streaks, about 1-2 pixels in width and are usually independent of the "seeing" conditions during the observation period.

Most objects in an astronomical image are only a few pixels and are characterised by a gaussian-like intensity profile rising above the average background intensity. Consequently, astronomical models have been based on these characteristics.

The classical vision model[18], whereby objects were defined by their edges, was first applied to astronomical imagery. Though algorithms used for this model were fast and performed well in poor fields, it required accurate computation and was only suitable to detect small objects. Also, its main disadvantage was that edges were also found for flaws, as well as stars. Besides, astronomical sources cannot be recognised by their edges but only from their intensity profiles.

The classical astronomical model is based on an image, $I(x,y)$, that is constituted by a slowly variable background with superimposed small scale astronomical objects which are associated to a point of maximum intensity. Then,

$$I(x, y) = ap(x, y) + \mu \tag{Eq. 4.1}$$

where

- a = the amplitude of the object
- $p(x,y)$ = the profile of the model object
- μ = the mean of the background variation

Astronomical sources are defined by their radial profiles and are characterised by a circular, bivariate gaussian profile. Hence,

$$p(\Delta x, \Delta y) = e^{-\frac{(\Delta x^2 + \Delta y^2)}{2\sigma^2}} \tag{Eq. 4.2}$$

where

- $\Delta x, \Delta y$ = the distance from the centroid of the object, and
- $\sigma \propto$ the size of the astronomical object taken as the full width at half magnitude(FWHM).
 $= \frac{FWHM}{2.36}$

over the range $-3\sigma < \Delta x, \Delta y < 3\sigma$

This is derived from the consideration that stars and other astronomical sources are point sources or have a dirac function. Most object detection projects, e.g. DAOPHOT, NEO Project at O.C.A, have adopted this model. However, this model has also proved to be inadequate for a complete and

comprehensive analysis due to the consideration of only a single scale for the algorithms used for detection. This led to the introduction of a multi-scale astronomical model as an extension of the classical astronomical model.

The multi-scale astronomical model is based on the splitting of the image into a space scale, allowing objects of different sizes to be detected. This concept arises from observations of sky images where small stars can be seen to be embedded in larger structures, the larger structures themselves being embedded in still larger ones, and so on. It is on this model that the detection task sequence for the NEO project has been based on. However, as asteroids are the only objects of interest, analysis using a single scale would suffice.

4.2 The NEO Detection Task Sequence

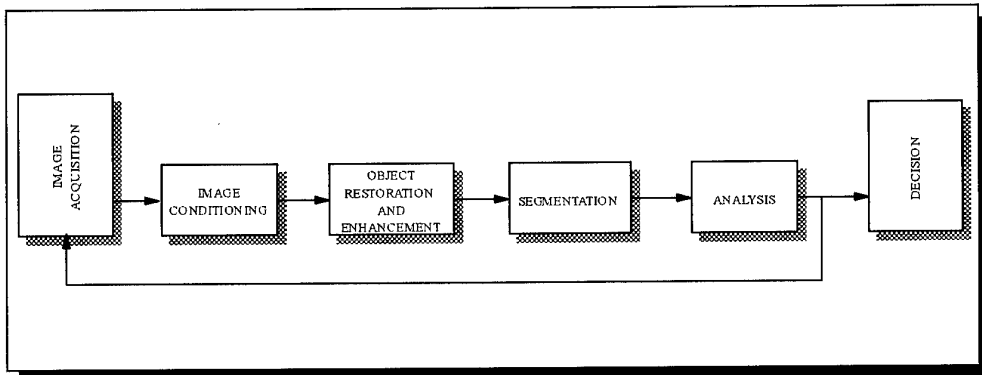


Fig 4.1 NEO detection task sequence

The NEO detection task sequence can be seen to be comprised of a sequence as illustrated in Fig. 4.1. Image acquisition was referred to in the previous chapter, and has been added in the task sequence to provide a more complete representation for the task sequence. The loop-back in the figure, elucidates the need for the repetition of image conditioning, object enhancement, segmentation, and analysis for frames of the same field, during the scan sequence, that are required to be obtained in order to classify objects as NEOs.

4.2.1 Image Acquisition and Image Conditioning

Image acquisition is effectuated by the CCD controllers and the necessary operations have been discussed in sec. 3.2.1 and sec. 3.2.2. The CCDs may be used in several possible modes of scan. However, whichever the mode of operation CCD data is acquired line-by-line, across the direction of scan.

As each pixel in a line is read out and digitised, preprocessing is usually carried out to remove effects of characteristics that are specific to the sensor. Raw CCD image is hardly useful, due to the varying sensitivities of individual pixels. The given CCD pixel output of a 2048x2048 image, is proportional to the number of photons(#*photons*) incident on that pixel. Thus,

$$I(x,y) \propto \#photons_{x,y}$$

$$I(x,y) = k_{x,y} \times \#photons_{x,y} \quad (\text{Eq. 4.3})$$

where x and y is the height and width of the CCD image. To overcome this non-uniformity, flat-fielding is carried out where the CCD is exposed to a uniform source such as the dawn sky or the inside of the telescope dome to map variations among the CCD pixels. A uniform source implies the number of photons falling on each pixel is the same and hence each pixel should ideally give the same output. But since the gain constant, $k_{x,y}$, differs from pixel to pixel, $I_{flatfield}(x,y)$ will also differs from pixel to pixel. Therefore,

$$I_{flatfield}(x,y) = k_{x,y} \times \#photons_{flatfield}$$

Once the response of each pixel is obtained, observers can scale data by an amount determined from the flat-field exposure and thereby correct individual pixel sensitivity. This can be achieved by

$$I(x,y) = \frac{k_{x,y} \times \#photons}{I_{flatfield}(x,y)} = \frac{\#photons}{\#photons_{flatfield}} \quad (\text{Eq. 4.4})$$

Thus removing the effects of individual pixel gains, $k_{x,y}$ and the output becomes solely dependent on the number of incident photons.

Besides flat fielding, another pre-processing operation that is specific to the imaging medium rather than the problem domain is dark-fielding. This provides a correction for hole-electron pairs that are thermally generated. Therefore, the normalised CCD output, $I_N(x,y)$ becomes

$$I_N(x,y) = \frac{k_{x,y} \times \#photons}{I_{flatfield}(x,y)} - I_{darkfield}(x,y) \quad (\text{Eq. 4.5})$$

4.2.2 Object Restoration and Enhancement

The task of enhancement is essential in improving image quality to aid in the accuracy of further processing. Following the classical astronomical image model defined by Eq. 4.1 and Eq. 4.2, the objective of this task is to restore and enhance the acquired image.

Image restoration is achieved by removing the effects of the optical system and atmospheric effects defined by a point spread function(PSF) and the background noise. Noise removal is usually achieved by using stationary filters having low pass characteristics and is effective if and only if the spectrum reaches essentially frequencies that are higher than the highest resolution feature of the objects to be detected. Hence, the use of a gaussian-shaped spatial filter would be ineffective as it offers the characteristics of a low pass filter. With such a filter, objects found in the high frequency range will be smeared and degraded. Such a smoothing operation is possible in background regions and at the edges of galaxies but is ineffective for stars and the halos of galaxies, as they have basically high frequency components .

Before object analysis and recognition can be carried out, object would have to be enhanced above background variation. Since asteroids and star-like objects are in the high frequency range, enhancement may be achieved by using high pass filters which enhances the resolution features and suppresses long wave fluctuations. However, the highest frequencies are also the most affected by noise. Therefore, these filters also enhance these noise components.

The filter for an astronomical image would then have to be a bandpass filter, $p'(x,y)$, such that the restoration would provide the amplitude, a or a value as close to it as possible. Thus,

$$\Sigma \Sigma p'(x,y)I(x,y) = a \quad \text{(Eq. 4.6)}$$

where $p'(x,y) = f(p(x,y))$

The value of $p'(x,y)$ can be determined by the method of least squares using a gaussian model for $p(x,y)$ to give a matched filter. Due to the characteristics of the filter (i.e. gaussian-like in intensity profile), if there is a star image centred at a pixel, $I(x,y)$ then the fit of the matched filter will be good at that point. The central height of the filtered image, $I_f(x,y)$ will then be proportional to the brightness of the star. If a star image is not present then the central height of $I_f(x,y)$ will be close to zero or even negative. Thus, a location in the image where the central height of $I_f(x,y)$ is a large positive value that probably lies near the centre of the star image.

Since the gaussian model($p(x,y)$) is dependent on object size, taken to represent "seeing" conditions, these filters must be adapted to each exposure, based on the size of a reference star estimated by its full width at half magnitude(FWHM). These principles have been followed in the DAOPHOT and NEO project at O.C.A. The NEO project at O.C.A uses a filter with a profile of a "Mexican hat", defined as the second derivative of a gaussian function.

4.2.3 Segmentation

The task of segmentation involves the separation of an input image into its constituent parts or objects such that objects of interest can be labelled and differentiated from other objects and from background pixels. This is very much dependent on the characteristics of the image, hence, the need for the previous steps to enhance these characteristics. Objects need to be separated as individual objects before they can be analysed to be able to make a decision. Ideally, pixels belonging to the same object have to be connected to form a single object definition.

Segmentation can be achieved sufficiently by thresholding, followed by a location of the centroid of detected objects. The threshold value can be determined by considering the fluctuations in amplitude due to the filtering operation. Since, the amplitude after filtering is given by Eq. 4.6. Then

$$\sigma^2(a) = \Sigma \Sigma \sigma^2(I(x,y))p'(x,y)$$

$$\sigma^2(a) = \mu \Sigma \Sigma p'(x,y) = \mu I$$

if a Poisson distribution of noise is considered. For effective detection, the threshold should then be set at approximately,

$$a > k\sigma(a)$$

with $k \approx 3$. Hence,

$$a > 3 \times \sqrt{\mu I}$$

Values of k may be taken dependent on the required error margins. Higher values of k may result in detection failures (failure to detect faint objects that could be classed as NEOs) while lower values may result in detection errors (detection of false objects).

As discussed in the previous sections, at regions where stars or star-like objects, the enhanced central points are equivalent to the points of maxima on each object. All determined points of maxima in the full image can then be considered and labelled as a possible asteroid. These points of maxima should be determined as accurately as possible, to about 1/100th of a pixel, since even minute errors could introduce significant errors during astronomical co-ordinate reduction and on follow-up operations.

4.2.4 Analysis

The task of analysis provides a proper representation and description of the detected objects for subsequent processing. Parameters of interest in the field of astronomy for the description of a objects are those related to object intensity magnitude and object intensity profile characteristics.

Object intensity magnitudes can be represented in conjunction with its intensity profile by determining the second order geometric moments about the centre (given by the point of maximum at x_c, y_c) of the detected object. The geometric moments of order (p+q) of $f(x,y)$ are defined as

$$M_{p,q} = \sum \sum (x - x_c)^p (y - y_c)^q I(x,y)$$

where x and y are the co-ordinates of the object's pixels in the image.

The object profile may be represented by determining the major and minor axes of the object's intensity profile. This may be determined by solving for the following equation,

$$\frac{A}{B} = \sqrt{\frac{\dot{x}^2}{\dot{y}^2}}$$

$$\pi AB = \sqrt{16\dot{x}^2\dot{y}^2}$$

where \dot{x}^2 and \dot{y}^2 are the moment centroids of order 2 in x and y

$$\dot{x}^2 = \sum_x \sum_y (x - \bar{x})^2 I(x,y)$$

$$\dot{y}^2 = \sum_x \sum_y (y - \bar{y})^2 I(x,y)$$

Other intensity profile descriptors include

- a. the aspect ratio : the ratio of the objects major axis length to the minor axis length
- b. asymmetry : the rms fractional change in an object's intensity profile when reflected through its minor axis
- c. uniformity : rms deviation of an object's intensity profile, along its major axis, from a template object of the same size and the same mean intensity
- d. goodness to fit : the rms deviation of the object's intensity profile from a template object of the same size, orientation and peak intensity, normalised to the peak intensity of the object.

Most of these parameters have been used by the Spacewatch program and by the NEO project at O.C.A. Another scheme that could also be used in detecting streaks, that are made by fast moving

asteroids. Operators like the Hough transform could then be utilised for the analysis to locate straight lines that would indicate the presence of streaks.

Based on the outputs at this stage, components of the problem domain have now been suitably extracted to allow decisions to be taken over on the representations to provide adequate solutions.

4.2.5 Decision

Decisions resulting from recognition of possible NEOs are achieved by the comparison of images from the same area of sky to extract objects that could be an asteroid. Asteroids can be differentiated by their motion at almost constant velocity through space. Hence, at this stage a further classification of detected objects can be performed by marking static and non-static objects which can then be further classified as asteroids or dubious objects.

Before classification can be undertaken, errors due to telescope pointing errors and atmospheric refraction will not cover precisely the same region of sky, and hence, would have to be compensated. A stationary object will not appear at precisely the same location in an image due to these errors. However, the change in position is the same for each stationary object in the same scan. Registration can be achieved by determining the offset for a known stationary object in each frame and these errors can be easily compensated for wherever the entries from two images have to be compared.

Classification may be achieved either by the use of a database of symbolic data referring to properties of detected objects or by an image comparison. The use of databases offer a considerable advantage in that it offers a reduction of processed data from numerical to symbolic data. However, with image comparison methods redundant information present in object-less regions result in unnecessary overheads in processing.

Whichever the scheme, the basic recognition operations are similar. The main objective of the algorithm is to determine motion in objects and then verify if this motion is achieved at constant velocity. This is achieved by a comparison of two to three separate frames of the same field, taken after given a period of time, to locate objects that are present in all three and are steadily moving across the field.

Firstly, lists of detected objects in frames are made by segmentation and analysis. Objects that are not present at similar locations in either of the two lists of detected objects are classified as non-static objects. On comparison with the list generated from a third image of the same area differentiation of possible asteroids from other dubious objects can be made. When only two scans of the same field are

PROPRIETY INFORMATION

obtained a standard star catalogue¹² may be used to isolate non-stationary objects. The second frame can then be used to determine whether the object was moving at constant velocity.

The search area to be considered is made by assuming that since moving asteroids are assumed to have a constant velocity, the change in co-ordinates should be more or less a constant and the search area should increase linearly from the second to the third frame. The orbital elements of these recognised asteroids are calculated and then used to further classify them into specific classes of asteroids e.g. Amor, Aten, or Apollo etc.

¹²Star catalogue : catalogued collection of all known stars

5

CONCLUSION

The previous chapters have discussed the NEO detection problem; section 2 revealed the solution requirements for NEO detection as a whole, section 3 showed the functional requirements of the detection systems and section 4 discussed the algorithmic requirements.

The need of an NEO detection programme is definitely an essentiality in view of the possible cataclysmic consequences resulting from an asteroid impact. Through simulations of a whole-sky survey was seen that large telescopes, like the Schmidt telescopes, would offer large sky coverage in excess of about 6,000 to 10,000 square degrees/month, and at fainter limiting magnitudes (of up to a limiting magnitude of 24) were necessary to achieve adequate detection completeness. Whole-sky coverage may be increased by using already existing large telescopes around the world, all integrated into a network. Also, after detection, quick follow-up capabilities should also be possible, if confirmations and recovery of these detections are to be made. To provide such capabilities, detection should be achieved in real time.

5.1 The NEO Detection System

The NEO detection system was seen to comprise of 7 major blocks in Fig 3.1: the sensors, the acquisition unit, the NEO system controller, the image storage unit, the NEO detection engine, the host and the user-interface. Based on the requirements discussed for such a system in section 3, an massively parallel processor based NEO detection system can be represented as in Fig. 5.1

Based on the required properties for a good imaging medium, as stated in sec.3.1.1, it was seen that charged coupled devices far out-classed photography as a suitable surveying sensor. By arranging CCD chips in a mosaic, large surveying efficiencies could be achieved. The number of CCD chips that make the mosaic is dependent on the size of the telescope focal plane. For the Schmidt telescope with a 30cm focal plane, the most cost-effective solution would be a staggered arrangement of CCD chips (9 for the Loral chips and 16 for the Kodak chips) in two rows, perpendicular to the direction of scan as seen in Fig 5.1. Two rows are adequate because of the mode of scan that would most likely be used i.e. the sidereal scan. However, at the expense of a more complicated control, astronomical co-ordinate reduction and image registration, two or three such rows may be used to avoid the repetition of scans as mentioned in sec 3.2.1.3.

A dedicated, high speed processor with a crystal controlled master clock is required to provide the necessary stable timing waveforms, via shaping(driver) circuits to control the CCD chips. For large

CCD arrays, bi-directional read-out techniques may be used. However, this is only possible in the stare mode. Digital signal processors chip (e.g. TMS320C40) may be used as the processor since these processors usually have high speed communication and computation characteristics. Preamplification and analog-to-digital conversion would then be carried out on acquired CCD data. Data transfer rates expected can be much higher than 10 Mbytes/sec for large CCD arrays depending on the mode of scan that is used, as seen in Table V. This requirement on speed can be reduced by using local multi-channel controllers to service a subarray of a few CCD chips simultaneously. The TMS320C40, for example, has six independent channels and can handle combined data rates well in excess of 10 MBytes/sec. A collection of independent multi-CCD controllers can then be used to handle data acquisition for a large CCD array and offer the possibility of real-time operation.

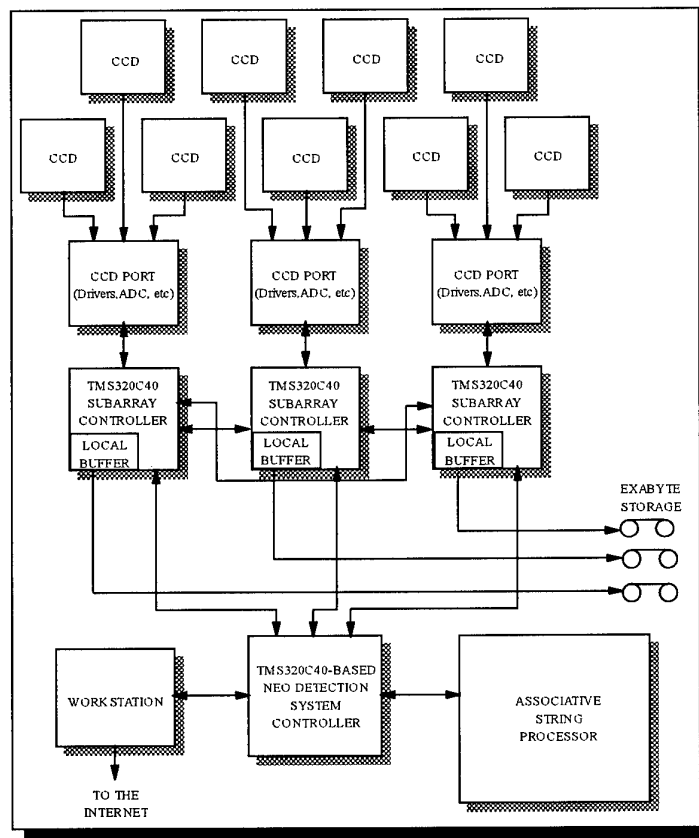


Fig. 5.1 Implementation of an NEO Detection system based on TMS320C40 DSP chips

Buffers would then store acquired data, as independent frames, before they are processed. Dual buffers schemes would be necessary to provide simultaneous access to the data and the buffers by the CCD controller and detection engine. The multi-CCD controller should store complete frames before switching to the other buffer. The size of each buffer would be dependent on the number of CCDs serviced. A system as in Fig. 5.1 would require a dual buffer of at least 50 Mbytes¹³. Data archiving

¹³ 50 Mbytes = 3 CCDs (3x2048x2048) x 2 bytes (16 bits) x 2 (dual buffer)

facilities should also be provided. Secondary storage of acquired data may be provided by Exabyte tapes via SCSI interfaces to the subarray controller.

A multi-channel, global array control, by a TMS320C40-based NEO detection system controller, provides the synchronisation and control for the local TMS320C40 subarray acquisition controllers as illustrated in Fig.5.1. It should also provide the detection engine access to the local acquisition buffers. The array controller would have to provide detection-buffer access in order for processing to be completed in about 12-240 sec depending on the mode of scan used.

The Associative String Processor(ASP) serves as the detection engine. For real-time NEO detection, high performances demands of much more than 0.5 TeraOPS (as seen in the simple task sequence in section 3.1.3), can definitely be expected. The ASP appears to satisfy non-functional requirements of size, weight, power and cost as is required for a performance machine in the astronomical environment. The cost-effectiveness of the ASP on size, weight, power and cost has been summarised as,

performance/size ratio	: 10 Tera-OPS/ft ³
performance/weight ratio	: 0.1 Tera-OPS/lb
performance/power ratio	: 0.1 Giga-OPS/W
performance/cost ratio	: 1 Mega-OPS/\$

A Unix-based workstation e.g. a Helwett Packard 747i workstation, may be used as the host and for the user-interface. Results after processing should then be sent to the workstation for further confirmation, if necessary, and also to make results available to the astronomical community via the Internet.

5.2 The NEO Detection Task Sequence

The detection philosophy is based on the multi-scale astronomical model with astronomical objects, having a gaussian-like profile, in a slowly variable background as discussed in section 4.1. The task sequence comprises of image acquisition, image conditioning, object restoration and enhancement, segmentation, analysis and decision as shown in Fig. 4.1.

Image acquisition is carried out line-by-line from each CCD before temporary storage in buffers. This acquired data has to be conditioned to normalise CCD pixel sensitivities and thermal noise removal as seen in section 4.2.1. This task can be done on-the-fly during acquisition.

Object restoration and enhancement is achieved by the use of a stationary, bandpass filter. The intensity profile of the filter is in the shape of a "Mexican hat" that is gaussian-like. The size of this filter is dependent on "seeing" conditions at the time of CCD exposure and hence can vary from frame to frame. This would influence the point spread function of the observation. Mask sizes of 3x3 (during perfect conditions and the reference star having a FWHM of 3) to a possible maximum of 31x31 (during poor conditions and the reference star having a FWHM of about 24) can be expected.

The result of the filtering may be positive or negative values (due to the band-pass characteristics of the filter) with a decimal precision of up to 3 decimal places. Segmentation is achieved by thresholding filtered values above a value determined from the coefficients of the filter as seen in section 4.2.3. Objects are then located by their point of maxima with co-ordinates.

Each segmented object is then analysed to obtain characteristic features of its intensity magnitude and profile. This may be characterised by the moments of the object, its major and minor axes, aspect ratio, asymmetry, uniformity, goodness to fit etc. Streaks made by fast moving asteroids may also be detected by operations like the Hough transform. At this point, objects are defined in symbolic rather than numeric form.

Once symbolic representation and analysis of detected objects is achieved on three successive scans of the same field, the registration between frames of the same field and comparison of object characteristics can be made. Asteroids may be classified out by their property of constant velocity motion across observed fields. Comparison with the first two successive frames of the same field, non-stationary objects may be differentiated from stationary objects. On comparison of these non-stationary objects with the third frame of the same field, constant velocity may be used as a criteria to further classify objects as asteroids. Further astronomical co-ordinate reductions on these asteroids would then be required to classify these asteroids as possible near-Earth objects.

5.3 Future Work

Based on the NEO detection algorithms that have been researched, work at Aspex Microsystems Ltd, Brunel University, will concentrate in the implementation of these algorithms and task sequence on the ASP System Test-bed for Research and Applications (ASTRA) to show the suitability of the ASP as the detection engine. Efficiency studies on the implemented algorithms will be made to determine the final requirements and configuration of the final ASP-based NEO detection system.

REFERENCES

- [1] McFadden, L., Chapman, C.R. *Near-Earth Objects: Interplanetary Fugitives*, Astronomy, Aug 1992
- [2] Scotti, J.V., Rabinowitz, D.L. Marsden, B.G. *Near miss of the Earth by a small asteroid*. Nature, Vol.354, Nov 1991.
- [3] Morrison, D. . *The Spaceguard Survey: Report on the NASA International Near-Earth Object Detection Workshop*. Jan 1992
- [4] Verschuur, G.L. *The End of Civilisation*. Astronomy. Sept. 1991
- [5] Rabinowitz, D.L. *Detection of Earth-approaching asteroids in near-real time*. The Astronomical Journal. Vol. 101, No.4 . April 1991
- [6] Janesick, J. Blouke, M. *Sky on a chip: The fabulous CCD*. Sky and Telescope. Sept 1987
- [7] Maury, A. *Programme de decouverte De Nouveaux Petits Corps Du Systeme Solaire*. Report
- [8] Janesick, J. Elliot, T. *History and Advancements of Large Area Array Scientific CCD Imagers*. Astronomical Society of Pacific Conference Series, 1991
- [9] *An Introduction to the Imaging CCD Array*. Tektronics Technical Note, 1987
- [10] Leach, R.W. *Design of a CCD Controller Optimised for Mosaics*. Publications of the Astronomical Society of the Pacific. Oct 1988
- [11] Gunn, J.E., Emory, E.B., Harris, F.H., Oke, J.B., *The Palomar Observatory CCD Camera*, Publications of the Astronomical Society of the Pacific. June 1987
- [12] Richmond, M.W., Treffers, R.R., Filippenko, A.V. *The Berkeley Automatic Imaging Telescope*. Publications of the Astronomical Society of the Pacific. Oct 1993
- [14] Maury, A. *Notes on NEO Detection Requirements*
- [15] Lea, R.M. *The ASP: A cost-effective parallel microcomputer*, IEEE Micro, Oct 1988
- [16] Lea, R.M. *A WSI Associative String Processor*, Journal of VLSI Signal Processing, Vol.2, pp. 271-285, 1991
- [17] Stetson, P.B., *DAOPHOT: A Computer Program for Crowded Field Stellar Photometry*. Publications of the Astronomical Society of the Pacific. Mar 1987
- [18] Bijaoui, A., *Astronomical Image Inventory by the Wavelet Transform*. Technical Report
- [19] Ardouin, J., *Point Source Detection based on Point Spread Function Symmetry*. Optical Engineering. Vol.32. No.9, Sept 1993
- [20] Lorenz, H., Richter, G.M., Cappaccioli, M., Longo, G. *Adaptive Filtering in Astronomical Image Processing: I. Basic Considerations and Examples*. Astronomy and Astrophysics Vol 227, 1993
- [21] Teh, C., Chin, R.T. *On Image Analysis by the Methods of Moments*. IEEE Trans. on Pattern Analysis and Machine Intelligence, Vol 10, NO. 4 July 1988